EUKARYOTIC CELL, Dec. 2003, p. 1304–1314 Vol. 2, No. 6
1535-9778/03/$08.00+0 DOI: 10.1128/EC.2.6.1304–1314.2003

Saccharomyces cerevisiae Histidine Phosphotransferase Ypd1p Shuttles between the Nucleus and Cytoplasm for *SLN1*-Dependent Phosphorylation of Ssk1p and Skn7p

Jade Mei-Yeh Lu, Robert J. Deschenes, and Jan S. Fassler*

Departments of Biological Sciences and Biochemistry, University of Iowa, Iowa City, Iowa 52242

Received 23 June 2003/Accepted 10 September 2003

Sln1p is a plasma membrane-localized two-component histidine kinase that functions as an osmotic stress sensor in *Saccharomyces cerevisiae*. Changes in osmotic pressure modulate Sln1p kinase activity, which, together with Ypd1p, a phosphorelay intermediate, changes the phosphorylation status of two response regulators, Ssk1p and Skn7p. Ssk1p controls the activity of the HOG1 mitogen-activated protein kinase pathway. Skn7p is a nuclearly localized transcription factor that regulates genes involved in cell wall integrity and other processes. Subcellular compartmentalization may therefore play an important role in eukaryotic two-component pathway regulation. We have studied the subcellular localization of SLN1 pathway components and find that Ypd1p is a dynamic protein with a role in shuttling the osmotic stress signal from Sln1p to Ssk1p in the cytosol and to Skn7p in the nucleus. The need to translocate the signal into different intracellular compartments contributes a spatial dimension to eukaryotic two-component pathways compared to the prototypical two-component pathways of prokaryotes.

An important aspect of regulation of many, if not all, eukaryotic signal transduction pathways is the subcellular localization or compartmentalization of signaling molecules. In *Saccharomyces cerevisiae*, the osmotic stress-regulated mitogen-activated protein (MAP) kinase Hog1p is predominantly cytoplasmic in unstressed cells but rapidly concentrates within the nucleus in response to hyperosmotic conditions (7). Nuclear accumulation depends on Hog1p phosphorylation by the cytoplasmic MAP kinase kinase Pbs2p (7, 31), interaction with the Ptp2 protein (which has been proposed to be a nuclear anchor [22]), and the presence in the nucleus of the Msn2p and Msn4p transcription factors, which are involved in the stress response (31). The nuclear localization of Msn2p and Msn4p is regulated by some of the more global consequences of exposure of cells to stress, such as changes in cyclic AMP levels (10). Like Hog1p, Msn2p and Msn4p lack an apparent nuclear localization sequence (NLS), and a localization mechanism based on cytoplasmic anchoring has been proposed (10). Another example of a transcription factor that relocates to the nucleus in response to stress is Yap1p. Nuclear accumulation of Yap1p is accomplished via modification of the Yap1p cysteine-rich domains in the presence of an oxidant, which perturbs the Yap1p interaction with the exportin Crm1p as well as other interactions that favor export (16, 38).

The HOG1 pathway is regulated by a two-component phosphorelay pathway that consists of a dimeric sensor-kinase, Sln1p; the histidine phosphotransfer (Hpt) molecule, Ypd1p; and two response regulators, Ssk1p and Skn7p (14, 18, 21, 28, 29). Sln1p autokinase activity is modulated in response to changes in osmotic pressure. The phosphoryl group is transferred from a histidine residue near the kinase domain of Sln1p to a conserved aspartate within the Sln1p receiver domain, from there to a histidine on Ypd1p, and finally to an aspartate residue of one of two response regulators, Ssk1p and Skn7p (Fig. 1A) (18, 29). Since activation of the HOG1 MAP kinase pathway requires unphosphorylated Ssk1p, the pathway is inactive under normal osmotic conditions by virtue of the presence of a basal level of phosphorylated Ssk1p. Hypertonic conditions reduce Sln1p pathway activity, allowing Ssk1p to accumulate in the unphosphorylated form and thus triggering the activity of the HOG1 pathway (21, 29). In contrast, hypotonic conditions and certain mutations (e.g., *fps1* or *sln1**) stimulate Sln1p pathway activity and cause hyperphosphorylation of both the Ssk1p and Skn7p response regulators (5, 18, 36). Skn7p is a DNA binding protein, and phospho-Skn7p activates expression of the mannosyltransferase gene *OCH1* and other genes, including but not limited to those involved in cell wall integrity and cell cycle progression (19; J. S. Fassler et al., unpublished data). Skn7p is also involved in the activation of oxidative stress response genes; however, Skn7p aspartyl phosphorylation is not required (18, 24).

The Ssk1p response regulator is expected to localize to the cytoplasm, since molecules in the HOG1 pathway, including HOG1, are cytoplasmic in unstressed cells. The Skn7p response regulator, in contrast, is nuclear (4, 30). Hence, a detailed molecular understanding of yeast two-component regulation must account for the subcellular localization of the molecules in the pathway. Phosphotransfer to the nuclear Skn7p response regulator requires at least the transient presence of other two-component molecules in the nucleus or movement of the Skn7 protein out of the nucleus. In this report we show that there are no apparent changes in Ssk1p or Skn7p localization in response to different types of stress. In contrast, we find that the histidine phosphotransferase, Ypd1p, is normally present in both cytosol and nucleus, suggesting that Ypd1p may be responsible for delivering the phosphoryl group

* Corresponding author. Mailing address: Department of Biological Sciences, University of Iowa, Iowa City, IA 52242. Phone: (319) 335-1542. Fax: (319) 335-1069. E-mail: jan-fassler@uiowa.edu.

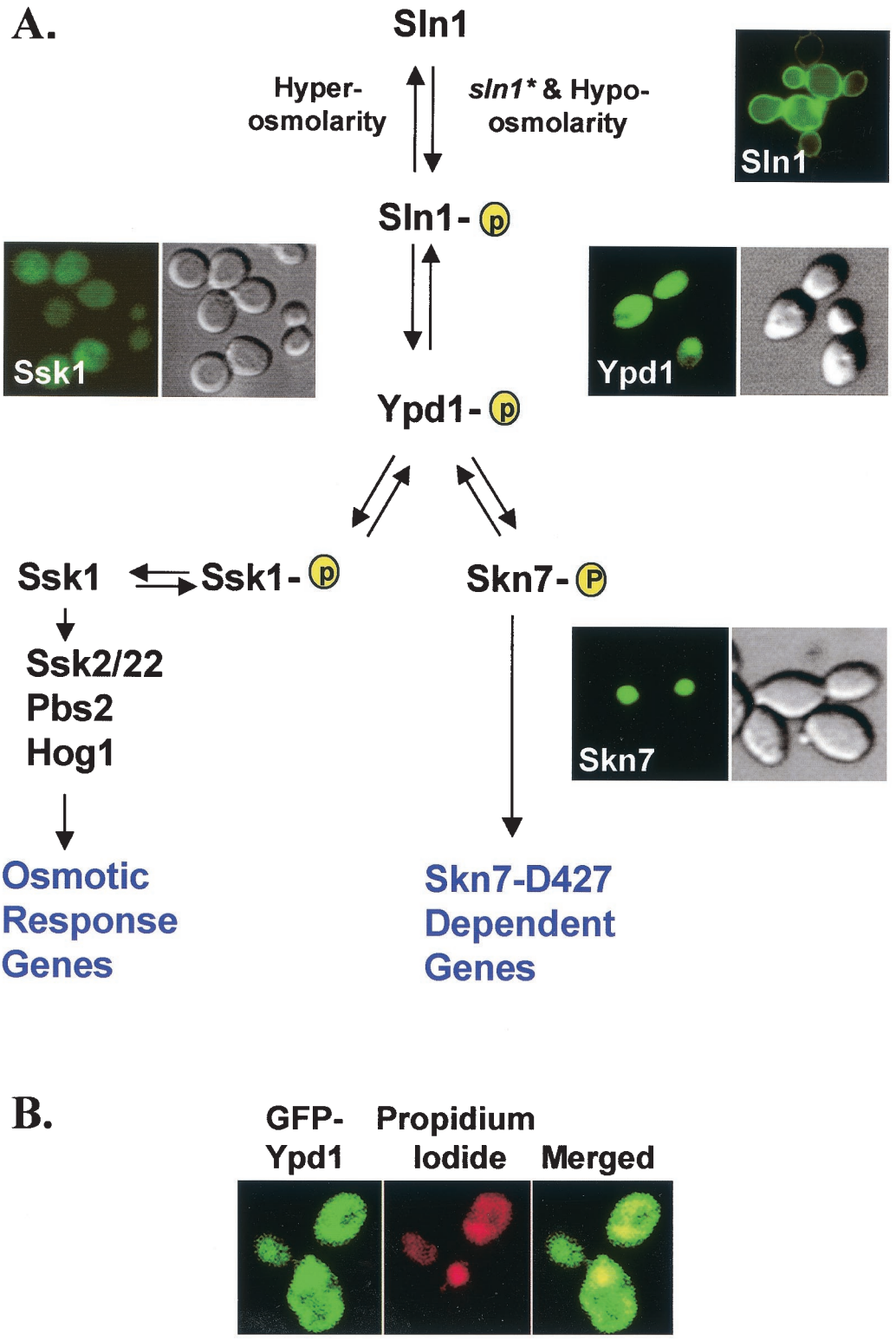

FIG. 1. SLN1 pathway components are compartmentalized in yeast. (A) Fluorescence microscopy of GFP fusions with Sln1p (pCLM814 in JF1455), Ypd1p (pJF1414 in JF2153), Ssk1p (pJL1465 in JF1919), and Skn7p (pJL1380 in JF1904). (B) Confocal microscopy of JF2153 (*ypd1*Δ) expressing GFP_{x2}-Ypd1p fusion protein. DNA was stained with propidium iodide. The merged image is shown on the right.

TABLE 1. Yeast strains used in this study

Strain[a]	Relevant genotype	Derivation (reference)
JF1455	*MAT***a**/α *his4-917 lys2-128*δ *trp1Δ1 ura3-52 leu2 sln1Δ::LEU2/SLN1*	Diploid strain
JF1565	*MAT*α *his3Δ200 leu2Δ1 ura3-52 trp1Δ63 lys2Δ201 can^R cyh^R*	Can^R Cyh^R derivative of FY834 (37)
JF1592	*MAT***a** *kar1-1 ade2-101 his4 leu2 trp1Δ1* or *-62 ura3-52*	
JF1904	*MAT*α *skn7Δ::TRP1 his3Δ200 leu2Δ1 ura3-52 trp1Δ63 lys2Δ201 can^R cyh^R*	*skn7Δ::TRP1* derivative of JF1565; one-step replacement
JF1910[b]	*MAT*α *sln1-22 his3Δ200 leu2Δ1 ura3-52 trp1Δ63 lys2Δ201 can^R cyh^R*	*sln1-22* derivative of JF1565; two-step replacement (36); plasmid free
JF1919	*MAT*α *ssk1Δ::LEU2 his3Δ200 leu2Δ1 ura3-52 trp1Δ63 lys2Δ201*	*ssk1Δ::LEU2* derivative of FY834; one-step replacement
JF1920[b]	*MAT*α *sln1-22 ssk1Δ::LEU2 his3Δ200 leu2Δ1 ura3-52 trp1Δ63 lys2Δ201 can^R cyh^R*	*ssk1Δ::LEU2* derivative of JF1910; one-step replacement
JF1974	*MAT*α *hog1Δ::TRP1 his3Δ200 leu2Δ1 ura3-52 trp1Δ63 lys2Δ201 can^R cyh^R*	*hog1Δ::TRP1* derivative of JF1565; one-step replacement
JF2123	*MAT*α *fps1Δ::LEU2 his3Δ200 leu2Δ1 ura3-52 trp1Δ63 lys2Δ201 can^R cyh^R*	Plasmid-free version of JF1732 (36)
JF2148	*MAT*α *his3Δ200 leu2Δ1 ura3-52 trp1Δ63 lys2Δ201 can^R cyh^R*; *pRS426-PTP2*	JF1565 carrying pRS426-*PTP2*
JF2150	*MAT*α *ypd1Δ::kan ssk1Δ::LEU2 his3Δ200 leu2Δ1 ura3-52 trp1Δ63 lys2Δ201*	*ypd1Δ::kan* derivative of JF1919; one-step replacement
JF2153	*MAT*α *ypd1Δ::kan his3Δ200 leu2Δ1 ura3-52 trp1Δ63 lys2Δ201 can^R cyh^R*; *pRS426-PTP2*	*ypd1Δ::kan* derivative of JF2148; one-step replacement
JF2219[b]	*MAT*α *sln1-22 ypd1Δ::kan ssk1Δ::LEU2 his3Δ200 leu2Δ1 ura3-52 trp1Δ63 lys2Δ201 can^R cyh^R*	*ypd1Δ::kan* derivative of JF1920; one-step replacement

[a] All strains used in this study except JF1455 were created by transformation of FY834 (37) or its *can^R cyh^R* derivative JF1565, both of which are isogenic to S288C. The JF1455 strain is congenic with S288C.

[b] *sln1-22* is one of several activating alleles of *SLN1* collectively referred to as *sln1** alleles. The *sln1-22* mutation causes a change of proline 1148 to serine (5).

to Ssk1p in the cytosol and to Skn7p in the nucleus. The presence of Ypd1p in both the cytosol and the nucleus may reflect the need for simultaneous phosphorylation of the Ssk1p and Skn7p response regulators under normal growth conditions.

MATERIALS AND METHODS

Strains. All strains used are isogenic and derivatives of S288C. Strains were constructed for these experiments or are from the Fassler laboratory collection (Table 1). Disruption of *YPD1* was achieved by transforming yeast with a PCR fragment containing a kanamycin resistance gene amplified with disruption oligonucleotides YPD-KAN-F (5′-TTGAATACCGGAGATATAATTCGTTTAT GCCACATAATCATCAATACATCATAGGCCACTAGT-3′) and YPD-KAN-R (5′-ATCTACACCTTAACCAATAATGAGTTATAGAGGAGCAAT GCAAAATCTAGCCAGCTGAAGCTT-3′), corresponding to the *YPD1* region from position −291 to +714. Disruptions were confirmed by genomic PCR and subsequent restriction analysis of the amplified fragment. *ypd1Δ::kan* transformants of JF2148 bearing pRS426-*PTP2* were screened by sensitivity to fluoroorotic acid (FOA) before PCR and restriction analyses. *skn7Δ::TRP1* disruption was carried out as described previously (18). Deletion of the *SSK1* gene was achieved by one-step replacement with the *Pst*I-*Xba*I fragment from plasmid pDSS14 from H. Saito (28). To disrupt *HOG1*, JF1565 was transformed with a disruption fragment linearized from pGY150 (39) by *Bam*HI-*Cla*I digestion. Transformants were screened by sensitivity to 0.9 M NaCl before Southern hybridization analysis. JF2123 (*fps1Δ::LEU2*) is a plasmid-free derivative of JF1732 (36).

Media. Solid and liquid media were prepared as described by Sherman et al. (32) and included synthetic complete (SC) medium lacking one or more specific amino acids and rich medium (yeast extract-peptone-dextrose [YPD]). Yeast transformation was performed by a modified lithium acetate method (9, 13). Yeast strains were grown to log phase and streaked or spotted onto various media after serial dilution. The viability of *ypd1Δ* strains carrying pRS426-*PTP2* was assayed on SC medium containing 0.1% 5-FOA to test functional complementation by various *YPD1* plasmids. All plate assays were carried out at 30°C.

Stress treatment. All localization studies were carried out with log-phase cultures grown at 28°C. Green fluorescent protein (GFP) fusion plasmids were introduced into strains with deletions in the corresponding gene.

(i) Osmotic stress. Hyperosmolarity was achieved by adding sorbitol to 1 M or NaCl to 0.5 or 0.9 M to log-phase cultures. Samples were taken and fixed at 5, 15, 30, 60, and 90 min after addition of the osmoticum. A *HOG1*-GFP construct (7) was used as a control. Hypo-osmolarity was generated by using the *fps1* mutation (strain JF2123), which prevents glycerol efflux and causes accumulation of intracellular glycerol (20). We previously showed that the *fps1* mutation activates the SLN1-SKN7 pathway (36), and we conclude, based on these studies, that Sln1p kinase activity is increased under hypotonic conditions.

(ii) Heat stress. Log-phase cells expressing GFP-*SKN7* or GFP-*YPD1* were shifted to elevated temperature (37 and 42°C), and samples were taken at 5, 15, 30, 60, 120, and 180 min.

(iii) Oxidative stress. Log-phase cells expressing GFP-*SKN7* were treated with 0.6 or 1 mM *tert*-butylhydroperoxide (Sigma) or 0.05% hydrogen peroxide (Sigma), and samples were taken at 5, 15, 30, 60, and 90 min. Activation of the oxidative response gene *TRX2* was monitored in parallel to confirm the treatment conditions.

Plasmids. The plasmids used in this study are summarized in Table 2. Construction schemes are described below. The nucleotide positions are referred as + if downstream of the ATG start codon and as − if upstream. All PCR fragments were amplified by using the high-fidelity *Pfu* or Turbo *Pfu* DNA polymerase (Stratagene).

(i) Reporters. The *OCH1* reporter plasmid was created by subcloning a 3-kb fragment containing UAS_{OCH1} (−336 to +26)-*lac*Z from pZL1320 (19) into pRS314 by using *Eco*RI and *Sal*I sites to create pJL1416.

(ii) GFP fusions. The *SLN1*-GFP plasmid pCLM814 was constructed by insertion of a *Not*I fragment containing the GFP open reading frame (ORF) at the stop codon of YEplac112-*SLN1* (B812). The GFP fragment was amplified by PCR with oligonucleotides B568 (5′-TCAAGTCGCGGCCGCATGTCTAAAG GTGAAGAATTATTC-3′) and B569 (5′-ATGACAGTGCGGCCGCTTATTT GTACAATTCATCCATACC-3′) and GFP mut3 (S65G S72A, GenBank accession number U73901) as a template. The pCLM814 plasmid was shown to be functional by complementation of the 2:2 inviability phenotype in tetrads from the *sln1Δ/SLN1*$^+$ heterozygote, JF1455, into which it was transformed.

The 2 μm GFP-*SKN7* plasmid pJL1380 was constructed by insertion of the *SKN7* ORF downstream of UAS_{SKN7}-GFP (F64L S65T) cassette previously cloned into pRS425 (pJL1363). The pJF1380 plasmid was shown to be functional by complementation of the oxidative stress and hygromycin B sensitivities of a *skn7Δ* strain.

To construct the GFP-*YPD1* fusion, a *Bam*HI-*Nhe*I polylinker was engineered by PCR (QuickChange site-directed mutagenesis kit [Stratagene]) beyond the translation start site of *YPD1* in pCLM669 (a pRS316-*YPD1* plasmid) by using oligonucleotides YPD1 + 3 *Bam*HI-*Nhe*I-F (5′-GCGGATCCAGCTAGCGTC TACTATTCCCTCAGAAA-3′) and YPD1 + 6 *Bam*HI-*Nhe*I-R (5′-CGTGCT AGCTGGATCCCAGACATTATTGTGTGTAT-3′). A GFP PCR fragment

TABLE 2. Plasmids used in this study

Plasmid	Description[a]
pCLM814	YEplac112-UAS_{SLN1}-*SLN1*-GFP
HOG1-GFP	pRS416-*HOG1*-GFP (7)
pJL1363	pRS425-UAS_{SKN7}-GFP
pJL1380	pRS425-UAS_{SKN7}-GFP-*SKN7*
pJL1414	pRS316-UAS_{YPD1}-GFP_{x2}-*YPD1*
PJL1415	PRS316-UAS_{YPD1}-GFP_{x2}-*ypd1H64Q*
pJL1416	pRS314-*OCH1* (−336 to +26)-*lacZ*
pJL1419	pRS315-UAS_{YPD1}-GFP_{x2}-*YPD1*
PJL1429	PRS416-UAS_{YPD1}-GFP_{x2}-*ypd1H64Q*
pJL1433	pRS315-UAS_{YPD1}-GFP_{x2}-*YPD1* H64Q
pJL1437	pRS416-UAS_{YPD1}-GFP_{x2}-*YPD1*-C*aaX*(CCIIS)
pJL1440	pRS315-UAS_{YPD1}-GFP_{x2}-*YPD1*-C*aaX*(CCIIS)
pJL1441	pRS416-UAS_{YPD1}-GFP_{x2}-*YPD1*-S*aaX*(SSIIS)
pJL1447	pRS315-GFP_{x2}-*YPD1*-SaaX(SSIIS)
pJL1453	pRS316-UAS_{YPD1}-GFP-NLS_{x2}-GFP-*YPD1*
pJL1454	pRS315-UAS_{YPD1}-GFP-NLS_{x2}GFP-*YPD1*
pJL1456	pRS316-UAS_{YPD1}-GFP_{x2}-NES-*YPD1*
pJL1461	pRS315-UAS_{YPD1}-GFP_{x2}-NES-*YPD1*
pJL1465	pRS316-UAS_{YPD1}-GFP_{x2}-*SSK1*
pJL1514	pRS313-UAS_{GAL10}-GFP-NLS_{x2}-GFP-*YPD1*
pJL1532	pRS313-UAS_{GAL10}-GFP-*HTB1*

[a] All plasmids except *HOG1*-GFP (7) were constructed for this study. See Materials and Methods for construction details. Plasmids used solely as intermediates in various construction schemes are not listed here.

amplified by using primers GFP*Bam*HI *Bgl*II-F (5′-GGGATCCTGAGATCTA TGTCTAAAGGTGAAGAATT-3′) and GFP *Nhe*I-R (5′-CCAGCTAGCGAT ATCTTGTACAATTCATCCATACC-3′) was then digested with *Bam*HI and *Nhe*I and cloned to generate pJL1356, in which GFP is fused to the N terminus of the *YPD1* ORF. To create GFP_{x2}-*YPD1*, a 1.8-kb fragment containing the GFP_{x1}-*YPD1* (+3 to +1072) sequence was fused via synthetic *Bgl*II and *Sal*I sites downstream of GFP, thus replacing the *YPD1* ORF with GFP-YPD1 in pJL1356 and generating a pRS316-GFP_{x2}-*YPD1* plasmid called pJL1414. Plasmid pJL1414 was shown to be functional by complementation of the *sln1* ssk1*Δ *ypd1*Δ) and the inviability phenotype of JF2153 (*ypd1*Δ, pRS426-*PTP2*) on 5-FOA plates selecting against the presence of the *PTP2* plasmid.

The GFP_{x2}-*SSK1* plasmid pJL1465 was constructed by replacing the *YPD1* ORF and downstream sequence in pJL1414 with a PCR fragment containing *SSK1* (+3 to +2632) via *Nhe*I and *Sal*I sites.

The nonphosphorylatable (H64Q) *YPD1* allele was made by two-step PCR mutagenesis based on the method of Landt et al. (17). In round one, *YPD1* sequences from position +178 to +1072 were amplified with a forward primer encoding the H64Q mutation (YPD1 + 178F-H/Q) (5′-GACAATCTGGGCC AGTTTTTAAAGGGTTCT-3′) and the reverse primer YPD1 + 1072*Sal*I-R (5′-GAAGGATTCTGTCGACTTTGTTGGTAC-3′). The PCR product was used as the reverse primer for round two with forward primer YPD1-786 *Spe*I-F (5′-GAACATTTAAACTAGTGTGATTCAGG-3′) and pCLM669 (pRS316-*YPD1*) as the template. The 1.8-kb PCR product was purified, digested with *Spe*I and *Sal*I, and cloned into pRS416. The GFP-*ypd1*H64Q fusion was constructed by first amplifying the region encompassing the *YPD1* coding sequence (positions +3 to 1072) from pJL1429 with oligonucleotides YPD1 + 3*Bam*HI-*Nhe*I-F and YPD1 + 1072*Sal*I-R and then cloning the fragment into pRS315 at *Bam*HI and *Sal*I sites to create a promoterless plasmid, in which the H64Q mutation was confirmed by sequencing. Finally, an *Spe*I-*Nhe*I fragment containing UAS_{YPD1}-GFP_{x2} was inserted upstream of the *YPD1* coding region to create pJL1433, a mutant counterpart to pJL1414. GFP_{x2}-*ypd1*H64Q was also subcloned into pRS316 via *Not*I and *Sal*I sites to create pJL1415.

C*aaX* and S*aaX* fusions of *YPD1* were created by mutagenizing the stop codon of *YPD1* to create *Mlu*I and *Xba*I sites by using oligonucleotides YPD1 + 501*Mlu*I *Xba*I-R (5′-GCTCTAGACGCGTAGGTTTGTGTTGTAATATTTA G-3′ and YPD1-786 *Spe*I-F. The 3.2-kb fragment was digested with *Spe*I and *Xba*I and ligated into *Xba*I site of pRS416, resulting in pJL1436, in which the upstream *Xba*I site was destroyed upon fusion with the *Spe*I site and the downstream *Mlu*I-*Xba*I sites were intact for subsequent ligation. A fragment consisting of the last 43 amino acids of Ras2p, including the C*aaX* box (CCIIS) motif, was PCR amplified from plasmid pB701 (2) by using oligonucleotides RAS2 + 844 *Mlu*I-F (5′-GGGACGCGTGAATAATAATAGTAAGGCCGGTC-3′) and RAS2 + 969 *Xba*I-R (5′-GCTCTAGACTTAACTTATAATACAACAGCCAC CCG-3′). The 126-bp PCR product was digested with *Mlu*I and *Xba*I and fused behind the *YPD1* coding sequence in pJL1436, creating the GFP_{x2}-YPD1-C*aaX* construct pJL1437. Similarly a S*aaX*-containing fragment in which the CCIISS sequence at the C terminus of Ras2 was mutated into SSIIS was amplified by using oligonucleotides RAS2 + 844 *Mlu*I-F and RAS2m + 950 *Xba*I-R (5′-GCTCTAGACTTAACTTATAATAGACGAGCCACCCGATCCGCTCT-3′) (mutated bases are underlined). The PCR fragment was inserted into pJL1436 via *Mlu*I and *Xba*I sites to create pJL1441. The *Not*I-*Sal*I fragments of pJL1414, pJL1437, and pJL1441 were subcloned into pRS315 to obtain pJL1419, pJL1440, and pJL1447, respectively.

The NLS-*YPD1* construct pJL1453 was made by inserting a 0.24-kb *Bam*HI-*Bgl*II fragment from pGPKI-NLS (a gift from S. Green) (3) containing two tandem copies of the simian virus 40 NLS into the *Bgl*II site between the two copies of GFP in pJL1414. In the NES-*YPD1* fusion, the nuclear export sequence (NES) from PKI (33) was engineered between the second copy of GFP and the N terminus of *YPD1* in two steps. The GFP_{x2}NES cassette was amplified by using YPD1-786 *Spe*I-F and GFP-NES-*Nhe*I-R (5′-CCTGCTAGCGTAAGCTTTGT CTTGTTGATATCGAGGCCTGCTAGTTTCAGCGCTAATTCATTTTTGTA CAATTCATCCATGCC-3′) (encoding GMDELYKNELALKLAGLDINKTKL TLA). The 2.3-kb PCR product (UAS_{YPD1}-GFP_{x2}NES) was fused upstream of the *YPD1* coding sequence in pJL1414 via *Spe*I and *Nhe*I sites to create pJL1456 (GFP_{x2}-NES-YPD1). The NLS- and NES-tagged GFP-*YPD1* fusions were subcloned into pRS315 to create pJL1454 and pJL1461, respectively.

Galactose-inducible GFP constructs. The GFP-NLS_{x2}-GFP-YPD1 fragment was released from pJF1454 by use of *Bam*HI and *Sal*I and fused in frame at the *Bam*HI site downstream of the *GAL* promoter in pRS313-UAS_{GAL10} (5) to create pJL1514.

The control plasmid, GFP-*HTB1* (pJL1532) was created in two steps. An *HTB1* PCR fragment was generated by using forward primer HTB1 + 4 *Bam-BglII* (5′-TGGATCCTGAGATCTGCTAAAGCCGAAAAGAAACC-3′) and reverse primer HTB1 + 1007 *Sal*I (5′-GATCAGAGCTCGTCGACAAGGAA TACTGAAGTGCA-3′) and genomic DNA as the template. The PCR fragment was inserted behind GFP in an intermediate plasmid. The GFP-*HTB1* fragment was then subcloned into a derivative of pRS313-UAS_{GAL10} (5).

β-galactosidase assays. Yeast protein extracts were prepared by glass bead lysis from cultures grown at 30°C and harvested at a density of 10^7 cells/ml. Extracts were cleared by centrifugation in all cases. Activities were normalized to protein concentrations (23) and are the averages for at least four different transformants.

Yeast protein extracts and immunoblot analysis. Yeast cultures were grown to log phase in selective media. Cells were pelleted and resuspended in 10 mM Tris-50 mM EDTA, washed once in lysis buffer (50 mM Tris [pH 7.6], 140 mM NaCl, 0.1% Triton X-100, 5 mM EDTA, 1 mM dithiothreitol, 1 mM phenylmethylsulfonyl fluoride, and protease inhibitor cocktail [Sigma]), pelleted, and frozen at −80°C. The pellets were resuspended in lysis buffer and broken by vigorous vortexing in the presence of 425- to 600-μm-diameter glass beads (Sigma), and lysates were cleared by centrifugation and stored at −20°C. The protein concentration was determined by using the Bio-Rad Microassay. GFP protein levels were examined by using rabbit anti-GFP antibody and horseradish peroxidase-conjugated goat anti-rabbit immunoglobulin G antiserum (Sigma). Immune complexes were visualized by using the ECL enhanced chemiluminescence kit (Amersham Corp.).

Fluorescence microscopy. Log-phase yeast cultures expressing GFP fusions were fixed in 70% ethanol, washed and resuspended in phosphate-buffered saline (PBS), and stained with 0.5 μg of 4′,6′-diamidino-2-phenylindole (DAPI) (Sigma) per ml to visualize nuclei. Cells were observed with a Leica DM RBE microscope and a Leica 100× PL Fluotar 1.3 NA objective. Images were captured with a Photonic Science digital charge-coupled device camera system. Images were processed by using IP-LAB Spectrum software and edited in Adobe Photoshop.

For confocal microscopy, log-phase cells were fixed in cold 75% methanol, washed twice in PBS and three times in 2× SSC (0.3 M NaCl, 0.03 M sodium citrate [pH 7.0]), and treated with DNase-free RNase A (100 μg/ml) (Sigma) for 20 min at 37°C. Samples were then rinsed several times in 2× SSC and incubated with 500 nM propidium iodide (Molecular Probes) prepared in 2× SSC for 5 min at room temperature. Samples were washed five times and resuspended in 2× SSC prior to microscopy with an MRC-600 laser scanning confocal microscope (Bio-Rad).

Heterokaryon assay. The heterokaryon assay was modified from published protocols (8, 27). JF2153 (*ypd1*Δ*kan*) carrying a pRS426-*PTP2* plasmid as well as pJL1514 (pRS313-UAS_{GAL10}-GFP-NLS_{x2}-GFP-YPD1) was grown to late log phase in synthetic medium (2% glucose) before dilution into medium containing

2% raffinose as the sole carbon source. The culture was grown overnight to 10^6 cells/ml, and galactose was added to a final concentration of 2%. The culture was then grown for 3 h, washed three times in YPD (2% glucose), and resuspended in YPD for an additional 2 h of growth. Cells (2×10^7) were mixed with an equal number of JF1592 (*kar1-1*) cells from a YPD-grown log-phase culture. The cell mixture was concentrated on a 25-mm-diameter, 0.45-μm-pore-size nitrocellulose filter and incubated at 28°C for 2 h on solid YPD. Cells were washed from filters by gentle vortexing in a microcentrifuge tube containing 0.5 ml of YPD, collected by brief centrifugation, fixed in cold 80% methanol for 30 min, washed twice in PBS, and resuspended in DAPI (0.5 μg/ml in PBS). The nonshuttling control, JF1565 (wild-type strain) bearing pJL1532 (pRS313-UAS_{GAL10}-GFP-*HTB1*), was mated to *kar1-1* cells in the same manner.

RNA analysis. RNA samples were prepared by using a hot acidic-phenol method (1). Electrophoresis and blotting were performed as described previously (39). Hybridization was performed with PerfectHyb hybridization buffer (Sigma) as directed by the manufacturer. ^{32}P-labeled probes were prepared by using random primers with Prime-It random priming labeling kit (Stratagene) with fragments isolated from plasmids. The GFP ORF was derived as a 0.75-kb *Bam*HI-*Bgl*II fragment from pJL1414, and *ACT1* was isolated as a 3-kb *Eco*RI fragment from pYIP5-ACT1 (39). Blots were exposed to X-ray film, and radiolabeled bands were visualized by autoradiography. The GFP probe was removed from the blot by washing in 0.2× SSC–1% sodium dodecyl sulfate at 75°C for 3 h followed by a 0.1% sodium dodecyl sulfate–10 mM Tris (pH 7.5) rinse at room temperature prior to hybridization with the *ACT1* probe.

RESULTS

Ypd1p resides in both nuclear and cytosolic compartments. The subcellular localization of Sln1p, Ypd1, Ssk1p, and Skn7p was examined by using GFP fusions on high-copy (Sln1p and Skn7p) or low-copy (Ssk1p and Ypd1p) yeast expression plasmids under the control of the native promoters (with the exception of Ssk1p, which was expressed by using the stronger *YPD1* promoter). In all cases, expression of the GFP fusions from these plasmids was able to complement the phenotypes of the corresponding mutants (data not shown). Sln1p-GFP localized to the rim of the cell, consistent with the expected plasma membrane localization of the sensor kinase (Fig. 1A). In contrast, GFP-Skn7p was present exclusively in the nucleus. GFP-Ssk1p appears to be localized to the cytoplasm (Fig. 1A); however, the relatively weak intensity of the GFP-Ssk1p signal precludes our ruling out its presence in the nucleus. These observations suggest that phosphotransfer from Ypd1p to the two response regulators occurs in distinct intracellular compartments and that the localization of Ypd1p could be a regulated step in the pathway, as has been previously reported for plants (12).

Analysis of GFP_{x2}-Ypd1p revealed that the Ypd1p protein is distributed throughout the cytoplasm and in the nucleus under normal growth conditions. There is no evidence of plasma membrane localization, suggesting that its interaction with the plasma membrane-localized Sln1p is transient. Nuclear Ypd1p is seen as a more intense spot of fluorescence that coincides with the DAPI-staining material (Fig. 1A and 2) within the cytoplasm. The presence of Ypd1p in the nucleus was confirmed by confocal microscopy (Fig. 1B). Since two copies of GFP were fused in frame with Ypd1p, the resulting fusion protein was 74 kDa in size, which is too large for passive import into the nucleus. We therefore conclude that the presence of Ypd1p in the nucleus could be due to active transport.

Localization of Ypd1p and Skn7p is unchanged in response to osmotic stress. To determine whether localization of Ypd1p or Skn7p changes in response to fluctuations in osmotic pressure, cells carrying GFP_{x2}-*SKN7* and GFP_{x2}-*YPD1* were shifted

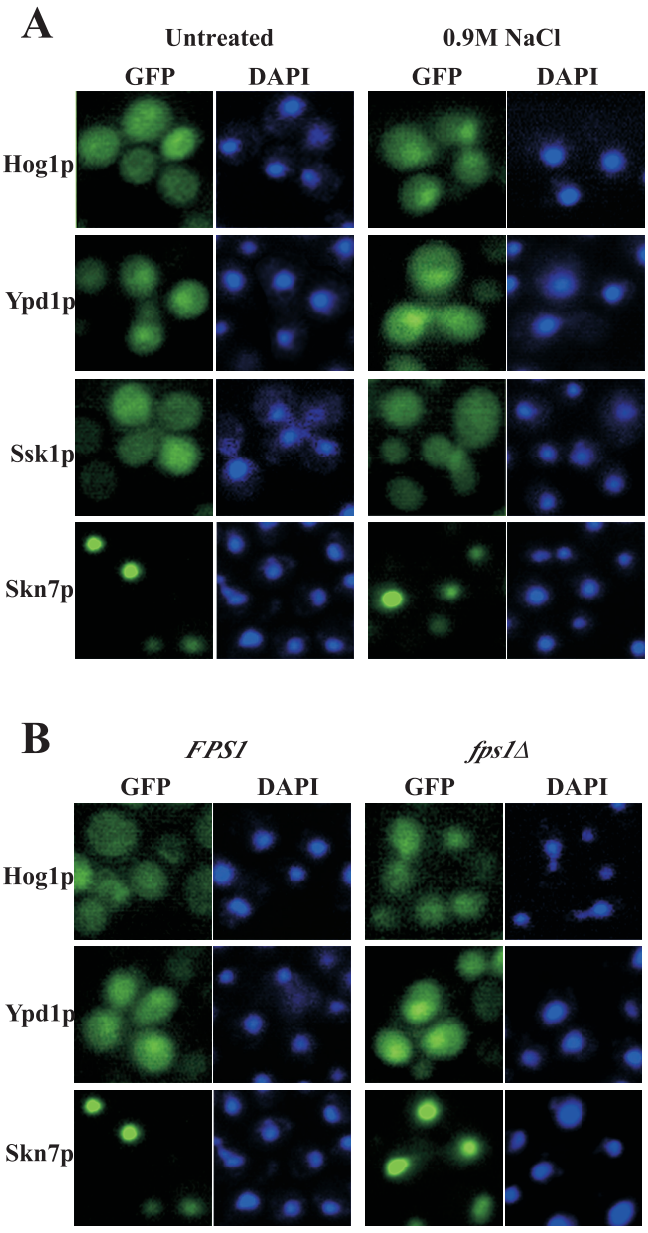

FIG. 2. Subcellular localization of Ypd1p (pJF1414), Ssk1 (pJL1465), and Skn7p (pJL1380) in response to changes in osmotic pressure. (A) Effects of one set of hyperosmotic conditions (0.9 M NaCl for 30 min). GFP-Hog1p (pRS416-GFP-HOG1, a gift from P. Silver) is shown as a control for osmotic stress-regulated nuclear localization. (B) The effect of hypo-osmotic stress in $FPS1^+$ (JF1565) and *fps1*Δ (JF2123) strains was compared.

to hyperosmotic medium. A *HOG1*-GFP construct was used as a control, since the rapid translocation of Hog1p to the nucleus upon exposure to a hyperosmotic stimulus has been well studied (7). As previously reported, Hog1p-GFP rapidly moved to the nucleus following salt addition; however, neither the GFP-Skn7p nor GFP-Ypd1p localization profile was altered following exposure of the cells to hyperosmotic conditions (Fig. 2A).

Skn7p undergoes Sln1p-dependent phosphorylation when cells are exposed to hypo-osmotic stress (19, 36). To examine the effect of a hypo-osmotic environment on localization, we

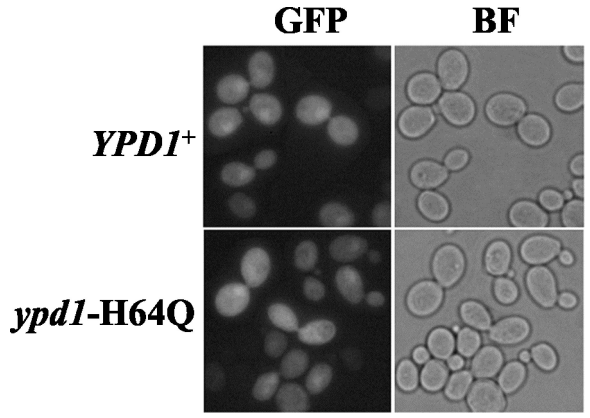

FIG. 3. Phosphorylation is not required for nuclear localization of Ypd1p. Fluorescence (left) and phase (right) microscopy of JF2153 (*ypd1*Δ) carrying GFP_{x2}-Ypd1p (pJL1419) or the nonphosphorylatable GFP_{x2}-Ypd1p-H64Q mutant (pJL1433). BF, bright field.

introduced a mutation in the *FPS1* gene, which encodes the major glycerol channel in yeast. Reduced glycerol efflux in the *fps1* mutant results in the accumulation of intracellular glycerol under normal growth conditions, which is interpreted by cells as a hypo-osmotic signal and increases activity of the SLN1-SKN7 pathway (20, 36). However, neither Hog1p, Skn7p, nor Ypd1p localization was affected in the *fps1* mutant (Fig. 2B). The effects of heat shock and oxidative stress, two conditions that activate Skn7p in an *SLN1*-independent fashion (15, 24, 30), were also examined. Again, no apparent changes in localization of Skn7p or Ypd1p were observed under these conditions (data not shown).

The Ypd1p localization profile is independent of phosphorylation. The Sln1p osmotic sensor is an integral membrane protein, and phosphotransfer from Sln1p to Ypd1p occurs on the cytoplasmic surface of the plasma membrane. Ypd1p is an obligatory intermediate in both the SLN1-YPD1-SSK1 and SLN1-YPD1-SKN7 pathways. The phosphorylation of Ypd1p might therefore play a role in its localization. To test this hypothesis, the histidine (H64) phosphoacceptor of Ypd1p was changed to glutamine. In comparisons of the wild type and the H64Q mutant, no differences were observed in the distribution of Ypd1p (Fig. 3), suggesting that Ypd1p localization to both cytosol and nucleus is not regulated by changes in osmotic pressure or by the phosphorylation state of the histidine.

Increased localization of Ypd1p to the nucleus or to the cytosol has no detectable effect on signaling. To test the hypothesis that movement of Ydp1p between the nucleus and the cytoplasm is important for phosphorylation of the response regulators residing in each compartment, an NLS or NES was added to the GFP_{x2}-*YPD1* construct. The effect of manipulating the localization of Ypd1p on Ssk1p phosphorylation was evaluated by looking at the viability of a *ypd1*Δ strain carrying the NLS- or NES-tagged *YPD1* construct and expressing *PTP2* from a high-copy *URA3*-marked plasmid. Phosphorylation of the Ssk1p response regulator is essential for viability; however, overexpression of the Hog1p phosphatase gene, *PTP2*, suppresses the phenotype (21, 25, 26). The ability of Ypd1p to phosphorylate Ssk1p is conveniently evaluated by testing for growth on medium containing 5-FOA, which selects against the presence of the *URA3*-marked *PTP2* plasmid.

NES tagged GFP_{x2}-Ypd1p was predominantly cytoplasmic (Fig. 4A), and a *ypd1*Δ strain carrying this construct was viable in the absence of the *PTP2* plasmid (Fig. 4B). As expected, the NLS-tagged GFP_{x2}-Ypd1p was predominantly nuclear (Fig. 4A). Surprisingly, nuclear localization of Ypd1p had no adverse effect on viability (Fig. 4B). This implies that Ssk1p was phosphorylated despite the apparent nuclear localization of Ypd1p.

The ability of the NES- and NLS-tagged GFP_{x2}-Ypdp1 to phosphorylate Skn7p was evaluated by measuring the activity of the *SLN1-SKN7*-dependent target gene reporter, *OCH1-lacZ* (19). Activating mutations in the *SLN1* gene (called *sln1** mutations) increase *OCH1-lacZ* expression 2.5- to 3-fold ((19) (Fig. 4C), and *sln1** activation is dependent on Skn7p phosphorylation, since mutation of the phosphorylated aspartate residue in the *SKN7* receiver domain abolishes SKN7-dependent activation of the reporter (19). *sln1** activation also depends on phosphotransfer from Ypd1p to Skn7p (18). In the presence of NLS-tagged Ypd1p, both Ypdp1 and Skn7p are present in the nucleus, and therefore *sln1** activation of the *OCH1-lacZ* reporter was normal, as expected (Fig. 4C). In the presence of the NES-tagged Ypd1p, which we found to be largely cytoplasmic, *sln1** activation was expected to be defective; however, no measurable decline in activation of a *SKN7*-dependent target gene was observed (Fig. 4C).

Tethering Ypd1p to the plasma membrane prevents signaling to Skn7p. The absence of observable effects of the NES and NLS Ypd1p tags on signaling might suggest that phosphotransfer between Ydp1p and the Ssk1p and Skn7p response regulators is not limited to any particular subcellular compartment. Alternatively, the results might reflect the presence of efficient native trafficking signals that allow Ypd1p to circulate in and out of the nucleus. To better discriminate between these possibilities, we tethered Ypd1p to the plasma membrane by using the C*aaX* box prenylation motif from Ras2p. Sequences containing a C*aaX* box prenylation motif were fused to the 3′ end of GFP-*YPD1.* A control construct (S*aaX*) in which the *CaaX* box cysteines were changed to serine, thus preventing plasma membrane localization, was also generated. Western analysis showed that each Ypd1p derivative was expressed at levels roughly comparable to that of the wild type (Fig. 5B, rightmost panel [data not shown for S*aaX* construct]). As expected, Ypd1p-C*aaX*, but not Ypd1p-S*aaX*, was partially localized to the plasma membrane. Some cytoplasmic staining is still apparent in the Ypd1p-C*aaX* strain, possibly reflecting trafficking intermediates (Fig. 5A). The ability of each construct to phosphorylate Ssk1p was assessed by examining viability. Strains carrying Ypd1p-C*aaX* or Ypd1p-S*aaX* were both viable, suggesting that tethering Ypd1p to the plasma membrane does not inhibit phosphotransfer to Ssk1p (Fig. 5B). A more quantitative analysis of Ypd1p phosphotransfer to Ssk1p was carried out by examining the effect of the C*aaX* and S*aaX* mutants on expression of the HOG1 pathway target, *GPD1*, after a shift to high-salt medium. The C*aaX* mutant exhibited 75% of wild-type induction, while the S*aaX* control was nearly normal at 94% (data not shown). Thus, the effect of Ypd1p tethering on SLN1-SSK1 pathway activity was minimal.

The ability of tethered Ypd1p to signal to nuclear Skn7p was

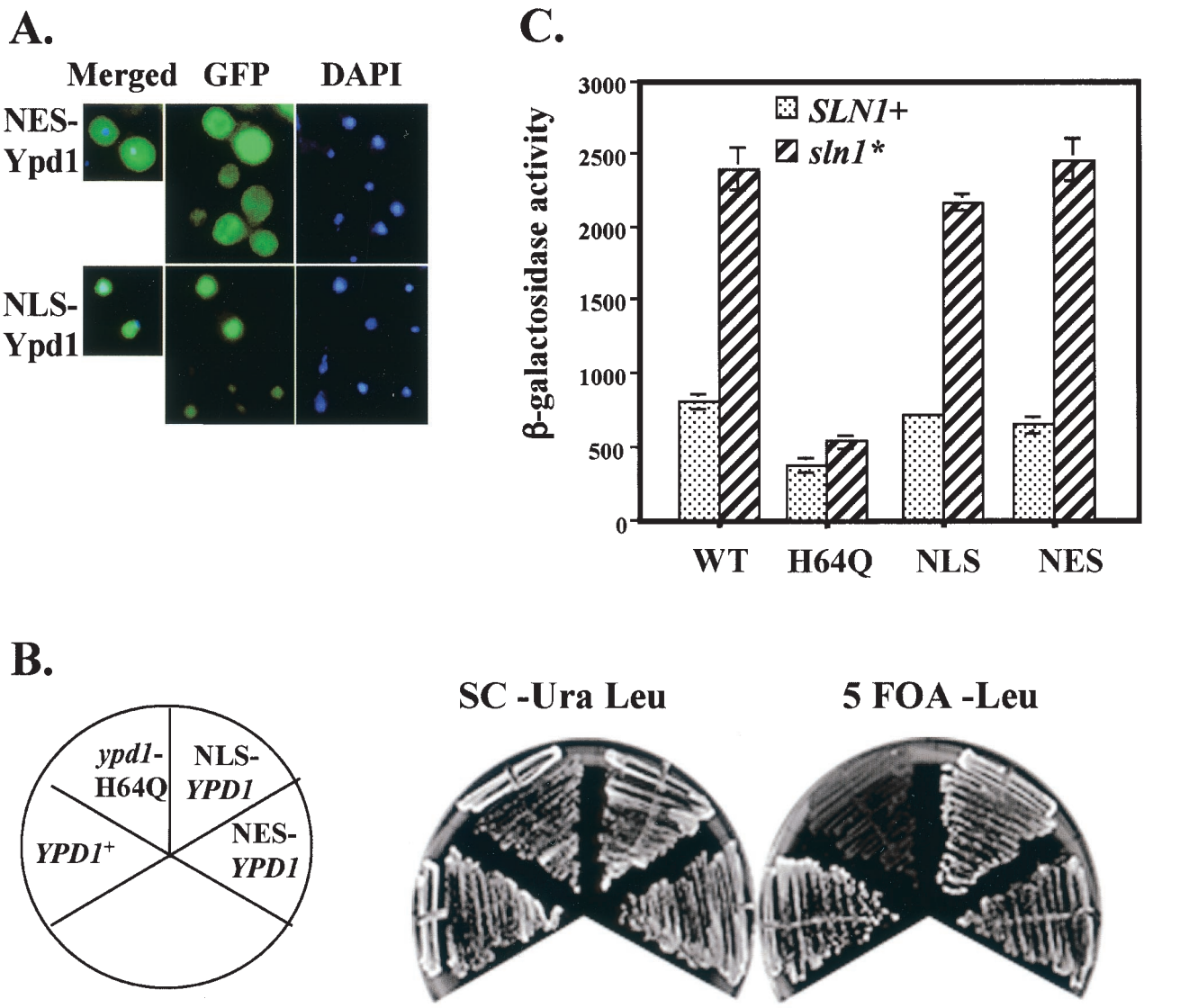

FIG. 4. Effects of NLS and NES tags on Ypd1p localization and function. (A) Localization of NLS (pJL1454)- versus NES (pJL1461)-tagged GFP_{x2}-Ypd1p. Merged GFP and DAPI images are shown at the left. (B) Effect of NES or NLS tags on Ypd1p signaling to Ssk1p. *YPD1* plasmids, including the wild type (pJL1419), H64Q (pJL1433), NLS (pJF1454), and NES (pJL1461) were introduced into JF2153, a *ypd1*Δ strain containing a 2 μm *PTP2* plasmid. Viability of the cells on 5-FOA medium reflects Ssk1p phosphorylation. (C) Effect of NLS and NES tags on Ypd1p signaling to Skn7p. *YPD1* plasmids, including the wild type (WT) (pJL1414), H64Q (pJL1480), NLS (pJF1453), and NES (pJL1456) in wild-type (JF2150) and *sln1** (*sln1-22*; JF2219) strains bearing the *SLN1-SKN7* dependent reporter, UAS_{OCH1}-*lacZ* (pJF1416) were assayed for β-galactosidase activity. Activities are the averages for four transformants. Error bars indicate standard deviations.

examined by assessing the effect of Ypd1p-C*aaX* on *sln1** activation. As seen previously, wild-type *YPD1* exhibited threefold activation in this assay (Fig. 5C), whereas the *ydp1 H64Q* mutant exhibited no activation. The *ydp1*-C*aaX* allele resembled the H64Q mutant in this assay, exhibiting no *sln1** activation. In contrast, the *YPD1*-S*aaX* construct was nearly fully active. These results indicate that nuclear localization of Ypd1p is necessary for signaling to Skn7p.

NLS-Ypd1p is capable of nucleo-cytoplasmic shuttling. The finding that nuclear targeting of Ypd1p is essential for Skn7p activation together with the lack of apparent effect of NLS and NES Ypd1p tags on signaling activity led us to propose that Ypd1p may shuttle between compartments to regulate Ssk1p and Skn7p. This was tested by using a heterokaryon assay (8). In this assay, a *kar1* mutant defective in nuclear fusion is mated with cells carrying a transcriptionally regulated NLS-tagged GFP-Ypd1 fusion protein. If the GFP fusion is capable of nuclear export, it will move out of the *KAR1* nuclei and into the *kar1* nucleus, causing GFP staining in both nuclei of the heterokaryon. The nuclear-localized NLS-tagged GFP-*YPD1* allele was placed under the control of the galactose-inducible *GAL10* promoter and transformed into a *ypd1*Δ strain kept alive by a *PTP2* overexpression plasmid. Expression of the NLS-tagged GFP-*YPD1* construct was highly inducible by galactose and was repressed within an hour of switching to glucose (Fig. 6B). Following mating with the *kar1-1* strain, the

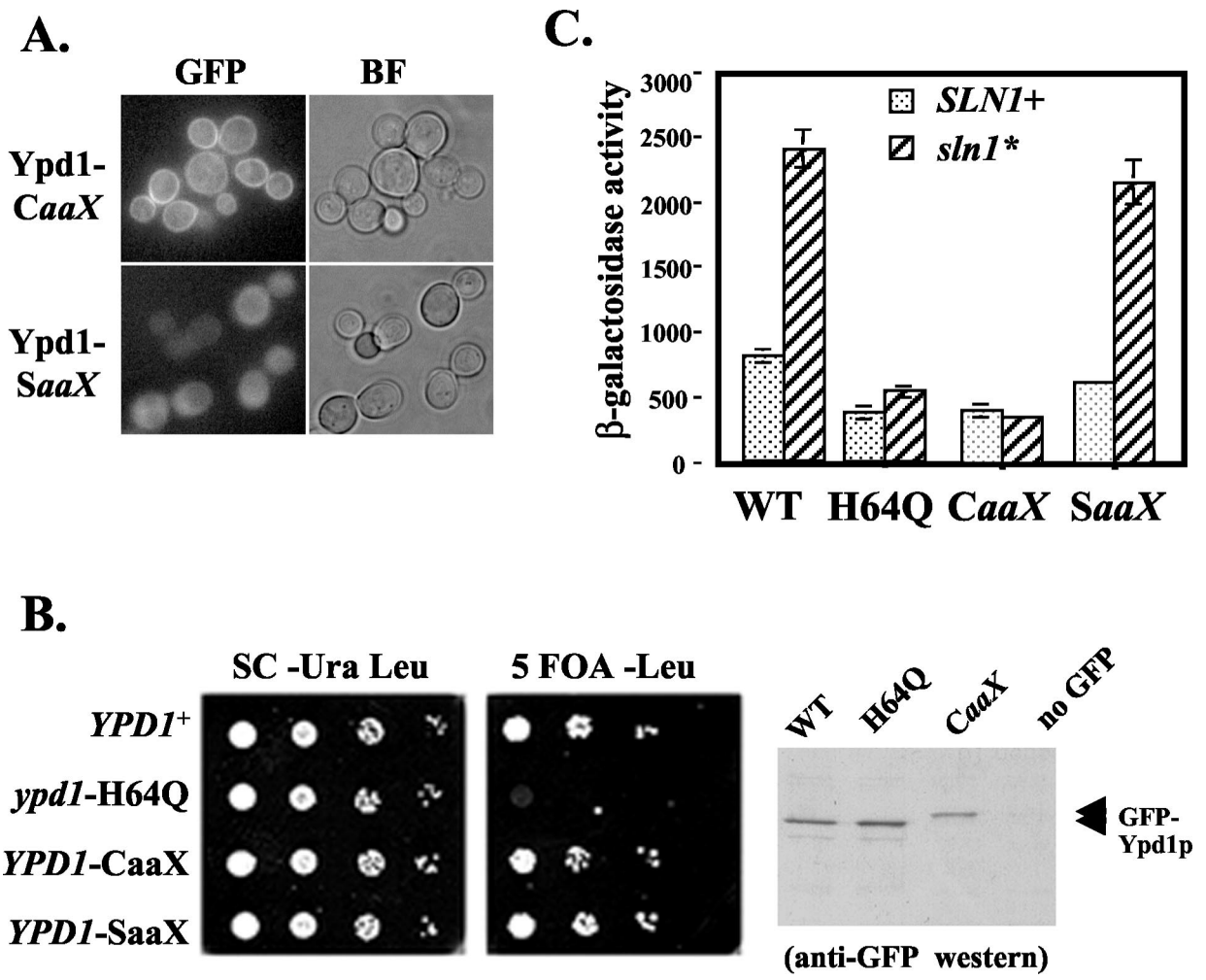

FIG. 5. Localization and function of plasma membrane-localized GFP-Ypd1p. (A) GFP fluorescence and bright-field (BF) images of cells carrying Ypd1p tagged with the Ras2p prenylation signal (C*aaX*; pJL1440) or the mutant prenylation signal (S*aaX*; pJF1447). (B) Viability assay measuring the ability of Ypd1p-C*aaX* to signal to Ssk1p. *LEU2*-marked *YPD1* plasmids (wild type [WT], pJL1419; H64Q, pJL1433; C*aaX*, pJF1440; and S*aaX*, pJL1447) were introduced into a *ypd1*Δ strain (JF2153) which is kept alive by the presence of a high-copy *PTP2* plasmid. Complementation is indicated by growth on 5-FOA, which selects against the *URA3*-marked *PTP2* plasmid. Western blot analysis showing similar levels of expression of the GFP-Ypd1p fusions is shown in the right panel. (C) Reporter assay measuring the ability of Ypd1-C*aaX* to signal to Skn7p. *URA3*-marked *YPD1* plasmids (wild type, pJL1414; H64Q, pJL1415; C*aaX*, pJF1437; and S*aaX*, pJL1441) in *SLN1* (JF2150) and *sln1** mutant (JF2219) strains bearing the *SLN1-SKN7* dependent reporter, UAS_{OCH1}-*lacZ* (pJF1416) were assayed for β-galactosidase activity. Activities are the averages from four transformants. Error bars indicate standard deviations.

majority of heterokaryons showed GFP fluorescence in both nuclei, indicating nuclear export of Ypd1p (Fig. 6A). In contrast, fluorescence from a GFP fusion with the yeast histone H2B gene (GFP-*HTB1*) was restricted to a single nucleus in control heterokaryons (Fig. 6A). These data strongly support the conclusion that Ypd1p moves between the nucleus and the cytoplasm.

DISCUSSION

Eukaryotic two-component pathways share many features with the more prevalent bacterial two-component pathway. However, some accommodations are assumed to be necessary due to the spatial constraints imposed by the compartmentalized intracellular environment. In this study we have examined the subcellular localization of the two-component signaling molecules in the yeast SLN1 pathway, and we conclude that the distribution of the histidine phosphotransfer protein, Ypd1p, in both the cytosol and the nucleus is one strategy by which eukaryotic two-component pathways have adapted to a compartmentalized environment.

The SLN1 pathway bifurcates downstream of the histidine phosphotransferase, Ypd1p, and culminates in the phosphorylation of two very different types of response regulators. Phosphorylation of the cytosolic response regulator, Ssk1p, is essential for viability, whereas phosphorylation of the nuclear response regulator, Skn7p, is not. Thus, the existence of separate nuclear and cytosolic pools of Ypd1p may be a reflection of the need to retain a pool of cytoplasmic Ypd1p even under conditions that call for Skn7p phosphorylation.

Under normal conditions, the small size of Ypd1p (19.2 kDa) may allow diffusion in and out of the nucleus. However, fusion of Ypd1p to two tandem copies of GFP did not alter the

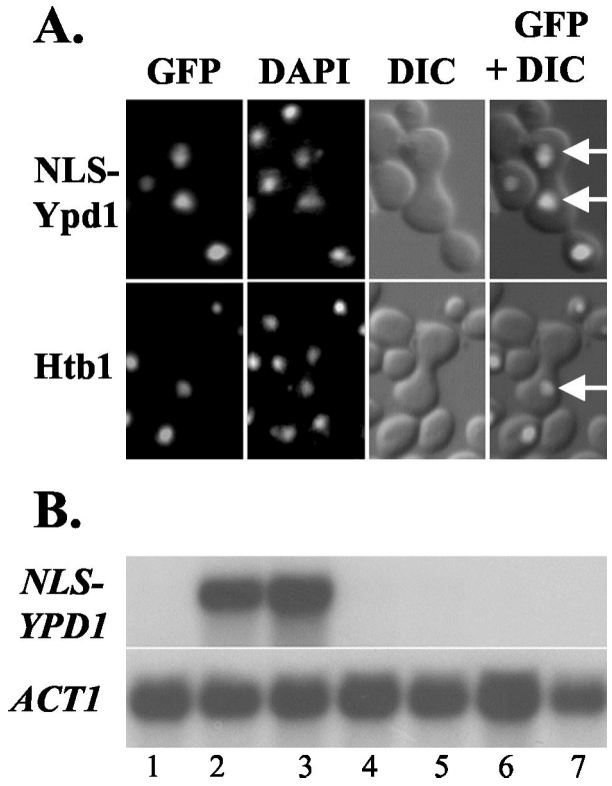

FIG. 6. GFP-NLS-Ypd1p migrates between nuclei in yeast heterokaryons. (A) Cells harboring a galactose-inducible GFP-NLS-*YPD1* (JF2153) (upper panel) or GFP-*HTB1* (JF1565) (lower panel) construct were mated with JF1592 (*kar1-1*) cells for 2 h. Arrows indicate heterokaryon nuclei. DIC, differential interference contrast. (B) Northern blot analysis of GFP-NLS-*YPD1* RNA expression during the time course of the heterokaryon assay (upper panel). *ACT1* RNA (lower panel) levels are shown as a loading control. Samples were from cultures in raffinose (lane 1), in galactose (1 and 1.5 h [lanes 2 and 3, respectively]), in glucose (1 and 2 h [lanes 4 and 5, respectively]), and during mating (1 and 2 h [lanes 6 and 7, respectively]). Twenty micrograms of total RNA was loaded per time point.

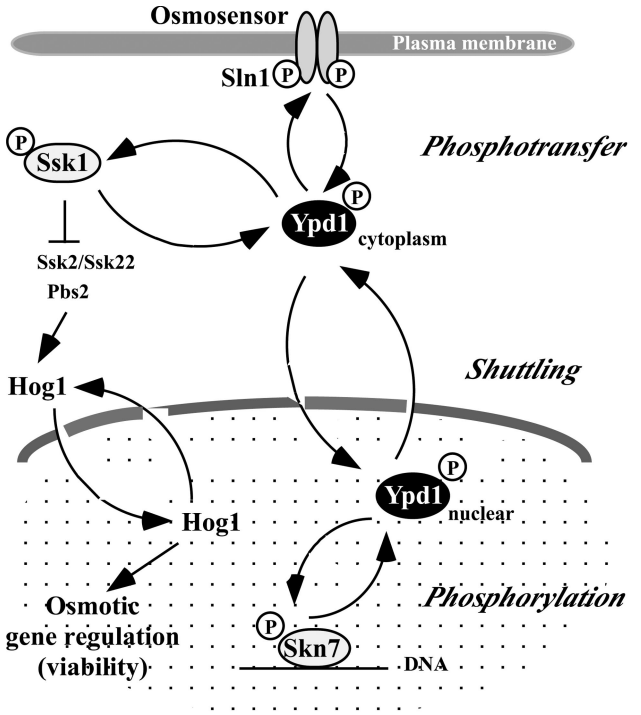

FIG. 7. Working model showing the multiple roles of Ypd1p in the osmotic response signal transduction pathway. Phosphotransfer, the transfer of a phosphoryl group from the receiver domain of Sln1 to the conserved histidine 64 in Ypd1p; shuttling, the movement of Ypd1p in and out of the nucleus. The diagram shows the translocation of the phospho form of Ypd1p; however, the dephospho form of Ypd1p may likewise be involved. Phosphorylation, the transfer of the Ypdp1 phosphoryl group to the conserved aspartates in the receiver domains of the nuclear Skn7p and cytoplasmic Ssk1p (not labeled) response regulators. Phosphorylation of Skn7p leads to activation of SLN1-SKN7-dependent gene expression, and phosphorylation of Ssk1p leads to negative regulation of the HOG1 MAP kinase cascade and the maintenance of viability.

pancellular distribution, suggesting the possible involvement of more active translocation mechanisms. When strong heterologous NLS and NES tags were added to the protein, the localization profile became nuclear in the case of the NLS fusion and cytoplasmic in the case of the NES fusion. These results suggest that any localization signals embedded within the Ypd1p sequence or present within proteins that normally interact with Ypd1p are relatively weak or that the strength of the intrinsic import and export signals are perfectly balanced, giving an even distribution of the protein both inside and outside the nucleus.

Even in the presence of strong NLS and NES signals, Ypd1p levels in the nucleus and cytosol were sufficient to sustain near-normal levels of signaling in both compartments. This suggests that very little Ypd1p is needed in each compartment or that the protein is very efficiently recruited to the appropriate signalasome. We used a heterokaryon assay to validate the conclusion that Ypd1p is capable of moving out of the nucleus in spite of the NLS tag. Heterokaryon assays were used first to demonstrate nuclear-to-cytoplasmic protein movement for Npl3p (8) and later to show nucleocytoplasmic shuttling of Gal80p (27) and Los1p (6). We conclude that native Ypd1p is fully capable of trafficking into and out of the nucleus to accomplish its dual signaling missions.

Although signaling to Ssk1p, as measured by viability and, quantitatively, by induction of a HOG1-dependent target gene, was not strongly affected when Ypd1p was plasma membrane associated, signaling to Skn7p was eliminated, presumably by curtailing the transit of Ypd1p to the nucleus. This is consistent with the view that Skn7p has a strict nuclear localization and that Ypd1p must enter the nucleus to carry out phosphotransfer with the Skn7p response regulator.

In our current working model for the spatial organization of the yeast two-component pathway molecules (Fig. 7), SLN1 pathway signaling is regulated by the intracellular shuttling of the phosphorelay intermediate Ypd1p and by the differential compartmentalization of the cytoplasmic Ssk1p and the nuclear Skn7p response regulators. In step one (phosphotransfer) of the pathway, plasma membrane-associated Sln1p transfers a phosphoryl group to the cytoplasmic Ypd1p. In step two (shuttling), phospho-Ypd1p translocates into the nucleus. In step three (phosphorylation), Ypd1p-P phosphorylates Skn7p in the nucleus as well as Ssk1p in the cytoplasm. This model is

supported by several lines of evidence. First, localization studies show the presence of Ypd1p in both the cytoplasm and the nucleus. Second, the fact that alteration of Ypd1p levels in either compartment by addition of NES or NLS tags had a minimal impact on signaling to Ssk1p or Skn7p suggests that even under these conditions Ypd1p is not confined to one compartment. Third, heterokaryon assays show that NLS-tagged Ypd1, and presumably native Ypd1p, is indeed capable of nuclear export. Finally, since tethering of Ypd1p to the plasma membrane via a *CaaX* box caused a severe impairment in Skn7p signaling, we conclude that Skn7p is restricted to the nucleus and that its activation requires nuclear targeting of Ypd1p. The temporal relationship of these events is not clear. Since the intracellular distribution of the nonphosphorylatable Ypd1p H64Q is indistinguishable from that of normal Ypd1p, it is possible that both phospho and dephospho forms of Ypd1p move in and out the nucleus. However, there is no known role for dephospho-Ypd1p in the nucleus.

An alternative model in which Ssk1p is phosphorylated inside the nucleus before moving out to the cytoplasm to regulate the HOG1 pathway seems unlikely, since Ssk1p appears to be cytoplasmically localized under all osmotic conditions tested. This localization pattern is consistent with the known cytoplasmic localization of the MAP kinase kinase, Pbs2p (7), which is activated by interaction with Ssk1p, and with the observation that the MAP kinase, Hog1p, translocates to the nucleus upon osmotic treatment. In addition, both the NES-Ypd1p and plasma membrane-tethered Ypd1-*CaaX* exhibited near-normal signaling to Ssk1p, indicating that nuclear Ypd1p is not required for Ssk1p signaling.

Recruitment of cytoplasmic signaling proteins into the nucleus is an essential step in the activation of gene expression in response to extracellular signals. In MAP kinase pathways, it is frequently the MAP kinase that transits to the nucleus. In eukaryotic two-component signaling, it appears that independent histidine phosphotransferase (Hpt) proteins such as Ypd1p may have evolved for this purpose. In *Arabidopsis thaliana*, *AHP1* to *-5* encode homologs of Ypd1p that function in the cytokinin signal transduction pathway (12, 34, 35). A subset of AHP molecules are translocated into the nucleus in a cytokinin-dependent manner, where they can signal to a nuclear family of response regulators (11). The regulated transport of the AHPs in *Arabidopsis* and the constitutive cycling of yeast Ypd1p into and out of the nucleus appear to represent distinct mechanisms for two-component signaling in compartmentalized cells. The basis for the difference between the two systems may lie with the tolerance and/or requirement of the cell for expression of pathway targets. For example, expression of cytokinin genes in the absence of cytokinins may be harmful, whereas modest expression of SLN1-SKN7 target genes such as *OCH1*, encoding a mannosyltransferase, is likely to be important even in the absence of stress. It will be of interest to examine the localization of molecules in other eukaryotic two-component pathways to determine whether Hpt-based translocation is a general principle in eukaryotic two-component signaling pathways.

ACKNOWLEDGMENTS

This work was supported by Public Health Service grant GM-56719 from the National Institutes of Health to J.S.F. and R.J.D. and by a postdoctoral fellowship from the American Heart Association to J.M.-Y.L.

Our appreciation goes to Pam Silver for the Hog1-GFP construct, to Steven Green for the GPKI-NLS plasmid, to W. Scott Moye-Rowley for the GFP antibody, to Kevin Campbell and members of his lab for use of the confocal microscope, to Michael Dailey for assistance with various nuclear staining protocols, and to Dan Weeks for help with *Xenopus*-based assays for examining localization.

REFERENCES

1. **Ausubel, F. M., R. Brent, R. E. Kingston, D. E. Moore, J. G. Seidman, J. A. Smith, and K. Struhl.** 1989. Current protocols in molecular biology. John Wiley and Sons, New York, N.Y.
2. **Bartels, D. J., D. A. Mitchell, X. Dong, and R. J. Deschenes.** 1999. Erf2, a novel gene product that affects the localization and palmitoylation of Ras2 in *Saccharomyces cerevisiae*. Mol. Cell. Biol. **19:**6775–6787.
3. **Bok, J., X. M. Zha, Y. S. Cho, and S. H. Green.** 2003. An extranuclear locus of cAMP-dependent protein kinase action is necessary and sufficient for promotion of spiral ganglion neuronal survival by cAMP. J. Neurosci. **23:** 777–787.
4. **Brown, J. L., H. Bussey, and R. C. Stewart.** 1994. Yeast Skn7p functions in a eukaryotic two-component regulatory pathway. EMBO J. **13:**5186–5194.
5. **Fassler, J. S., W. M. Gray, C. L. Malone, W. Tao, H. Lin, and R. J. Deschenes.** 1997. Activated alleles of yeast *SLN1* increase Mcm1-dependent reporter gene expression and diminish signaling through the Hog1 osmosensing pathway. J. Biol. Chem. **272:**13365–13371.
6. **Feng, W., and A. K. Hopper.** 2002. A Los1p-independent pathway for nuclear export of intronless tRNAs in *Saccharomyces cerevisiae*. Proc. Natl. Acad. Sci. USA **99:**5412–5417.
7. **Ferrigno, P., F. Posas, D. Koepp, H. Saito, and P. A. Silver.** 1998. Regulated nucleo/cytoplasmic exchange of HOG1 MAPK requires the importin beta homologs NMD5 and XPO1 EMBO J. **17:**5606–5614.
8. **Flach, J., M. Bossie, J. Vogel, A. Corbett, T. Jinks, D. A. Willins, and P. A. Silver.** 1994. A yeast RNA-binding protein shuttles between the nucleus and the cytoplasm. Mol. Cell. Biol. **14:**8399–8407.
9. **Gietz, R. D., and R. A. Woods.** 2002. Transformation of yeast by lithium acetate/single-stranded carrier DNA/polyethylene glycol method. Methods Enzymol. **350:**87–96.
10. **Gorner, W., E. Durchschlag, M. T. Martinez-Pastor, F. Estruch, G. Ammerer, B. Hamilton, H. Ruis, and C. Schuller.** 1998. Nuclear localization of the C_2H_2 zinc finger protein Msn2p is regulated by stress and protein kinase A activity. Genes Dev. **12:**586–597.
11. **Hwang, I., and J. Sheen.** 2001. Two-component circuitry in Arabidopsis cytokinin signal transduction. Nature **413:**383–389.
12. **Imamura, A., Y. Yoshino, and T. Mizuno.** 2001. Cellular localization of the signaling components of Arabidopsis His-to-Asp phosphorelay. Biosci. Biotechnol. Biochem. **65:**2113–2117.
13. **Ito, H., Y. Fukuda, K. Murata, and A. Kimura.** 1983. Transformation of intact yeast cells treated with alkali cations. J. Bacteriol. **153:**163–168.
14. **Ketela, T., J. L. Brown, R. C. Stewart, and H. Bussey.** 1998. Yeast Skn7p activity is modulated by the Sln1p-Ypd1p osmosensor and contributes to regulation of the HOG pathway. Mol. Gen. Genet. **259:**372–378.
15. **Krems, B., C. Charizanis, and K.-D. Entian.** 1996. The response regulator-like protein Pos9/Skn7 of *Saccharomyces cerevisiae* is involved in oxidative stress resistance. Curr. Genet. **29:**327–334.
16. **Kuge, S., N. Jones, and A. Nomoto.** 1997. Regulation of yAP-1 nuclear localization in response to oxidative stress. EMBO J. **16:**1710–1720.
17. **Landt, O., H. P. Grunert, and U. Hahn.** 1990. A general method for rapid site-directed mutagenesis using the polymerase chain reaction. Gene **96:**125–128.
18. **Li, S., A. Ault, C. L. Malone, D. Raitt, S. Dean, L. H. Johnston, R. J. Deschenes, and J. S. Fassler.** 1998. The yeast histidine protein kinase, Sln1p, mediates phosphotransfer to two response regulators, Ssk1p and Skn7p. EMBO J. **17:**6952–6962.
19. **Li, S., S. Dean, Z. Li, J. Horecka, R. J. Deschenes, and J. S. Fassler.** 2002. The eukaryotic two-component histidine kinase Sln1p regulates *OCH1* via the transcription factor, Skn7p. Mol. Biol. Cell **13:**412–424.
20. **Luyten, K., J. Albertyn, W. F. Skibbe, B. A. Prior, J. Ramos, J. M. Thevelein, and S. Hohmann.** 1995. Fps1, a yeast member of the MIP family of channel proteins, is a facilitator for glycerol uptake and efflux and is inactive under osmotic stress. EMBO J. **14:**1360–1371.
21. **Maeda, T., S. Wurgler-Murphy, and H. Saito.** 1994. A two-component system that regulates an osmosensing MAP kinase cascade in yeast. Nature **369:**242–245.
22. **Mattison, C. P., and I. M. Ota.** 2000. Two protein tyrosine phosphatases, Ptp2 and Ptp3, modulate the subcellular localization of the Hog1 MAP kinase in yeast. Genes Dev. **14:**1229–1235.
23. **Miller, J. H.** 1972. Experiments in molecular genetics. Cold Spring Harbor Laboratory, Cold Spring Harbor, N.Y.
24. **Morgan, B. A., G. R. Banks, W. M. Toone, D. Raitt, S. Kuge, and L. H. Johnston.** 1997. The Skn7 response regulator controls gene expression in the

oxidative stress response of the budding yeast *Saccharomyces cerevisiae*. EMBO J. **16:**1035–1044.
25. **Ota, I. M., and A. Varshavsky.** 1992. A gene encoding a putative tyrosine phosphatase suppresses lethality of an N-end rule dependent mutant. Proc. Natl. Acad. Sci. USA **89:**2355–2359.
26. **Ota, I. M., and A. Varshavsky.** 1993. A yeast protein similar to bacterial two-component regulators. Science **262:**566–568.
27. **Peng, G., and J. E. Hopper.** 2000. Evidence for Gal3p's cytoplasmic location and Gal80p's dual cytoplasmic-nuclear location implicates new mechanisms for controlling Gal4p activity in *Saccharomyces cerevisiae*. Mol. Cell. Biol. **20:**5140–5148.
28. **Posas, F., and H. Saito.** 1998. Activation of the yeast SSK2 MAP kinase kinase kinase by the SSK1 two-component response regulator. EMBO J. **17:**1385–1394.
29. **Posas, F., S. M. Wurgler-Murphy, T. Maeda, E. A. Witten, T. C. Thai, and H. Saito.** 1996. Yeast Hog1 MAP kinase cascade is regulated by a multistep phosphorelay mechanism in the Sln1-Ypd1-Ssk1 "two component" osmosensor. Cell **86:**865–875.
30. **Raitt, D. C., A. L. Johnson, A. M. Erkine, K. Makino, B. Morgan, D. S. Gross, and L. H. Johnston.** 2000. The Skn7 response regulator of *Saccharomyces cerevisiae* interacts with Hsf1 in vivo and is required for the induction of heat shock genes by oxidative stress. Mol. Biol. Cell **11:**2335–2347.
31. **Reiser, V., H. Ruis, and G. Ammerer.** 1999. Kinase activity-dependent nuclear export opposes stress-induced nuclear accumulation and retention of Hog1 mitogen-activated protein kinase in the budding yeast *Saccharomyces cerevisiae*. Mol. Biol. Cell **10:**1147–1161.
32. **Sherman, F., G. R. Fink, and J. B. Hicks.** 1986. Methods in yeast genetics, p. 163–167. Cold Spring Harbor Laboratory, Cold Spring Harbor, N.Y.
33. **Stade, K., C. S. Ford, C. Guthrie, and K. Weis.** 1997. Exportin 1 (Crm1p) is an essential nuclear export factor. Cell **90:**1041–1050.
34. **Suzuki, T., A. Imamura, C. Ueguchi, and T. Mizuno.** 1998. Histidine-containing phosphotransfer (HPt) signal transducers implicated in His-to-Asp phosphorelay in Arabidopsis. Plant Cell Physiol. **39:**1258–1268.
35. **Suzuki, T., K. Sakurai, A. Imamura, A. Nakamura, C. Ueguchi, and T. Mizuno.** 2000. Compilation and characterization of histidine-containing phosphotransmitters implicated in His-to-Asp phosphorelay in plants: AHP signal transducers of *Arabidopsis thaliana*. Biosci. Biotechnol. Biochem. **64:**2486–2489.
36. **Tao, W., R. J. Deschenes, and J. S. Fassler.** 1999. Intracellular glycerol levels modulate the activity of Sln1, an *S. cerevisiae* two-component regulator. J. Biol. Chem. **274:**360–367.
37. **Winston, F., C. Dollard, and S. L. Ricupero-Hovasse.** 1995. Construction of a set of convenient *Saccharomyces cerevisiae* strains that are isogenic to S288C. Yeast **11:**53–55.
38. **Yan, C., L. H. Lee, and L. I. Davis.** 1998. Crm1p mediates regulated nuclear export of a yeast AP-1-like transcription factor. EMBO J. **17:**7416–7429.
39. **Yu, G., R. J. Deschenes, and J. S. Fassler.** 1995. The essential transcription factor, Mcm1 is a downstream target of Sln1, a yeast "two-component" regulator. J. Biol. Chem. **270:**8739–8743.